

DETECTION OF ORTHOGONAL SINE AND COSINE PULSES BY LINEAR ACTIVE RC-NETWORKS

P. E. SCHMID, D. J. NOWAK

**Allen-Bradley Co.
Milwaukee, Wisconsin**

H. F. HARMUTH

Consultant

Summary An active RC matched filter, particularly useful for phase-coherent, coded or uncoded, binary or non-binary communication channels, is described. One detector circuit performs the equivalent of two simultaneous cross-correlations, avoiding the need for electronic multipliers, reference wave generation and phase synchronization. For example, only I circuits are needed in a receiver that is required to detect the polarity or presence of an orthogonal set of I sine and I cosine pulses.

In view of the circuits realizability with linear IC technologies, the sensitivities with respect to circuit component variations are analyzed in detail. The results of the sensitivity analysis are presented in graphical form. Experimental results confirm the predicted performance; i.e. Q-factors in excess of 4000 were obtained with small, general-purpose operational amplifiers.

Introduction Orthogonal sine and cosine pulses of duration T - consisting of 1, 2, ---M ... I integer cycles within the interval T - have been proposed and used for the transmission of digital information by several investigators.¹⁻³ In the parallel mode of operation, $2I$ independent binary digits may be transmitted simultaneously by multiplying each sine and cosine pulse by +1 or -1 and adding the multiplied pulses.' In the coded transmission mode, only one out of $2I$ signals is sent in one interval T .^{2,3} For the purpose of explaining the detector functions in a typical application, the parallel phase-coherent transmission mode will be referred to throughout this paper; however, it should be pointed out that the detector to be described can be utilized equally well for the reception of coded binary as well as nonbinary signals based on orthogonal sine and cosine pulses.

Principle of Operation In order to regain the binary digits at the end of each signal interval, two methods are commonly employed to perform the $2I$ necessary cross-correlations during each detection interval $0 \leq t \leq T$.⁴

Method A: Generate and synchronize $2I$ periodic reference waveforms and continuously multiply everyone of them with the received superposition of I sine and I cosine pulses. Integrate the $2I$ products during each detection interval and sample the integrated products periodically at the time $t = T$.

Method B: The composite pulse is fed into $2I$ linear filters with impulse responses approximating - as closely as possible - the above mentioned reference waveforms during each finite detection interval. Sample the $2I$ filters periodically at the instants $t = T$.

The detector circuit described in this paper improves on Method B and may be called a matched filter. Since a matched filter performs convolution rather than cross-correlation, the detector waveforms for Methods A or B are distinctly different within the detection interval; even so both methods yield the same result at the sampling instant $t = T$.

Filters “matched” for the pulses $\cos 2\pi Mt/T$ and $\sin 2\pi Mt/T$ call for impulse responses of the form $\cos(-2\pi Mt/T)$ and $\sin(-2\pi Mt/T)$, respectively, during each interval $0 \leq t \leq T$. Thus, the approach is based on the fact that sine and cosine pulses are eigenfunctions of the following differential equation and boundary conditions

$$\tau^2 \ddot{y} + y = 0, \quad y(0) = y(T), \quad \dot{y}(0) = \dot{y}(T) \quad (1)$$

where y stands either for voltage or current. A feedback circuit., consisting essentially of two active RC-integrators and an inverter stage, has frequently been used for the simulation of equation (1).⁵ One version of this circuit is shown in Fig. 1. It has the following attractive features:

1. One circuit simultaneously performs the convolution with both the sine and cosine pulse containing M cycles within the interval T . Thus only I circuits - rather than $2I$ - are needed in receiver structures such as given in references.¹⁻³
2. In comparison with Method A, the $2I$ electronic multipliers (with large dynamic range) are eliminated and the generation of $2I$ phase-synchronized reference waveforms is avoided.
3. The circuit is compatible with todays linear IC technologies.
4. Due to the absence of inductors, operation at frequencies as low as a fraction of a Hertz is feasible with Q - factors of several thousand.

It should be mentioned that the differential equation (1) is also obtained in a lossless LC-resonant circuit. A nearly lossless LC circuit has been used in the “Orthomatch” systems Orthomatch, however, did not operate in the phase-coherent mode, since one single LC-resonant circuit does not permit the simultaneous detection of both the sine and the cosine pulse. The performance of LC-resonant detectors is primarily determined by the inductors Q; thus, the size of high-Q inductors usually forbids the use of LC circuits at low frequencies. An electromechanical analog to the LC-resonant circuit has been used in the KINEPLEX system.⁷ Mechanical resonators have the advantage of small losses; on the other hand, they are not readily compatible with today's linear IC technologies.

Circuit Description and Analysis Fig. 1 shows the circuit for the detection of orthogonal sine and cosine pulses. An individual pulse with positive or negative polarity, or alternatively, the superposition of several pulses is applied to the input (e_1) at the time $t = 0$. At the time $t = T$, the voltages $e_3(T)$ and $e_4(T)$ are sampled for polarity decision and immediately after that, both capacitors C are discharged by closing the switches S_1 and S_2 . Then the next pulses can be detected. Resistors R_s represent the leakage resistance (incl. capacitor losses) between input and output of the operational amplifiers and also account for the finite dc-gain of the amplifiers. Beside RC-network drift, leakage and finite gain are the most significant limitations of the circuit.

The circuit of Fig. 1 is described by the following differential equation:

$$\tau^2 \ddot{e}_4 + 2\tau\lambda \dot{e}_4 + (1 + \lambda^2) e_4 = -(R_1/R_2) e_1 \quad (2)$$

$$\tau = RC(R_1/R_0)^{\frac{1}{2}}, \quad \lambda = (R/R_s)(R_1/R_0)^{\frac{1}{2}};$$

$$e_4 = e_4(t), \quad e_1 = e_1(t); \quad 0 \leq t \leq T.$$

$e_3 = e_3(t)$ is given by:

$$e_3 = -(R_0/R_1)^{\frac{1}{2}} (\tau \dot{e}_4 + \lambda e_4) \quad (3)$$

Since the homogenous solution of equation (2) is a damped sinusoidal oscillation of the form

$$e_4(t) = [A \cos t/\tau + B \sin t/\tau] \exp(-\lambda t/\tau),$$

the time required for $e_4(t)$ to decay to $1/e$ equals τ/λ and the cosine and sine terms will have $1/2\pi\lambda$ cycles in the interval $0 \leq t \leq \tau/\lambda$. Following a definition of Morris⁸ for the Q of RC circuits, one obtains $Q = (1 + \lambda^2)^{1/2} / 2\lambda$ for a circuit described by equation (2). In practice Q-factors of several thousand have been achieved (see experimental results).

Coarse tuning of the circuit is accomplished by proper selection of both integrator time constants RC. If the circuit elements associated with both integrators differ

($R'C \neq R''C''$; $R'_s \neq R''_s$), it can be verified that the basic relations (2) and (3) still hold by replacing τ^2 by $\tau' \tau''$, $2\lambda\tau$ by $\lambda' \tau'' \tau'$ and λ^2 by $\lambda' \lambda''$. Consequently, there is no need for precision RC networks and the “resonance time constant” τ may be easily adjusted by changing R_1 over a small range of its value. Note that an adjustment of the input amplitude by means of R_2 does not affect the tuning nor damping of the circuit. For simplicity, $R_1 = R_2$ is chosen in the following analysis.

In order to investigate the circuits detector operation, the input voltage e_1 in equation (2) is written as

$$e_1(t) = E \cos 2\pi Mt/T \quad \text{or} \quad = E \sin 2\pi Mt/T$$

It is assumed that the circuit is tuned for sine and cosine pulses with N cycles within the interval $0 \leq t \leq T$ i.e. $\tau = T/2\pi N$, with both N and M being integers. The solution of the differential equation for $e_3(t)$ and $e_4(t)$ at the time $t = T$ is straightforward but cumbersome. For the lossless circuit, i.e. for $\lambda = 0$, normalized output voltages are given in Table 1 for all eight possible cases.

Sensitivity Analysis A practical circuit will exhibit deviations from the ideal values indicated in Table 1. Therefore, the circuit designer will be interested in the magnitude of these deviations for any chosen set of circuit parameters. The two major causes for deviations, namely component value drifts and circuit damping, are introduced into the differential equations as follows:

1. Relative drift δ of the resonance time constant:

$$\begin{aligned} \tau &= RC, \text{ for } R_1 = R_0 \\ \tau &= T/2\pi N (1 + \delta) \end{aligned} \quad \delta = 10^{-5} \dots 10^{-2}$$

2. Circuit damping constant, for $R_1 = R_0$:

$$\lambda = R/R_S \quad \lambda = 10^{-8} \dots 10^{-2}$$

It is further assumed that the orthogonality interval of the incoming sum of sine and cosine pulses is synchronized with the detection interval.

For the indicated ranges of parameter variations, the solutions⁹ for $e_3(T)$ and $e_4(T)$ were programmed on a computer and the graphs of Figs. 2-5 show some of the computed deviations with respect to the ideal values in Table 1. Because performance deteriorations become more noticeable with increasing values of N , the graphs are shown for $N = 16$. Since the solutions for $e_3(T)$ and $e_4(T)$ are similar⁹ only the results obtained for $e_3(T)$ will be discussed here.

The numerical results are presented on double logarithmic paper in order to emphasize ranges of practical interest; deviations from the ideal values of $e_3(T)$ 1 or 0 of Table 1 are plotted vertically. The drift magnitude is plotted horizontally while λ is the curve parameter. Numerical results were obtained for both positive and negative values of δ ; the curves for negative δ are shown with dashed lines. A closer inspection of Figs. 2-5 reveals the following circuit performance criteria. Circuit component stability is the most critical factor for the rejection of the sine pulse $e_1(t) = E \sin 2\pi Nt/T$ at the “cos” output e_3 of Fig. 1. In this case (Fig. 3), λ is of little importance since the curves for $\lambda = 10^{-3}$ closely approach the nearly “lossless” curve for $\lambda = 10^{-8}$. However, circuit damping is most important for the rejection of the adjacent harmonic sine pulses with $M \neq N$ at the output e_3 of Fig. 1 (Fig. 5). As a rule of thumb, one may conclude that δ and λ are equally important. There is little point in making λ much smaller than δ or vice versa. For example, in a practical application utilizing 16 cosine and 16 sine pulses ($N = 1 \dots 16$), it is sufficient to keep both λ and δ below 10^{-3} in order to hold the crosstalk from an adjacent harmonic sine or cosine pulse below 2%.

Experimental Results Fig. 6A shows the sine pulse $e_1(t) = E \sin 2\pi t/T$, produced by digital/analog conversion circuits. Fig. 6B and C show the output voltages $e_3(t)$ and $e_4(t)$ caused by applying this sine pulse to the input of the circuit of Fig. 1. Correspondingly, Figs. 6D-F show a cosine pulse $e_1(t) = E \cos 2\pi t/T$ and the output voltages $e_3(t)$ and $e_4(t)$.

Typical oscillograms for measuring crosstalk are shown in Fig. 7. The sum of 16 sine and 16 cosine pulses with $M = 1 \dots 16$ is applied to a detector that is tuned for the pulses with $M = 8$, i.e. with a resonance time constant $\tau = T/2\pi \cdot 8$. In Figs. 7A,B,C the sum of all 32 pulses is received; but in Figs. 7D,E,F the sine and cosine pulses with $M = 8$ are omitted in order to demonstrate the negligible crosstalk from the other 30 orthogonal pulses. Figs. 7A,D show the composite input pulses while Figs. 7B,C and Figs. 7E,F show $e_3(t)$ and $e_4(t)$ for the two cases, respectively.

The circuits damping λ and Q-factor were determined by keeping the switches S_1 and S_2 open after exciting the circuit by a trigger pulse to oscillate. The impulse responses $e_3(t)$ or $e_4(t)$ were then observed. For an oscillation frequency of 100Hz, the experimental amplitude decay time τ/λ equalled about 14 seconds. Hence, about 1400 cycles occurred during the time τ/λ . From this follows:

$$\lambda = 1/(2\pi \cdot 1400) \approx 1.1 \cdot 10^{-4} \quad \text{and} \quad Q = (1 + \lambda^2)^{\frac{1}{2}}/2\lambda \approx 4400.$$

Finally, Fig. 8 shows responses of three detectors, tuned for the resonance time constants $T/(2\pi \cdot 128)$ and $T/(2\pi \cdot 129)$ and $T/(2\pi \cdot 130)$ to an input pulse $e_1(t) = E \cos 256\pi t/T$. With $T = 8$ ms the corresponding detector “resonance frequencies” were 1024Hz, 1032Hz and 1040Hz. Fig. 8A shows $e_3(t)$ at the first mentioned detector while Figs. 8B and 8C represent the output voltages $e_3(t)$ of the first adjacent and the second adjacent

detectors, respectively. The lower two traces reveal that the crosstalk from adjacent harmonic sine and cosine pulses is still negligible at the sampling instant.

Above results were obtained with small, general purpose solidstate operational amplifiers, having an openloop gain between 80 and 90 dB, as well as polystyrene capacitors and FET switches.

Conclusions

1. One detector circuit performs the equivalent of two simultaneous cross-correlations. Generation and synchronization of reference waveforms as well as electronic multiplication is avoided.
2. Fine tuning is easily accomplished with a single adjustment. No precision RC components have to be selected. Amplitude adjustment does not affect the tuning nor the damping of the circuit.
3. Experimental results confirm the calculated low crosstalk factors at resonance frequencies up to 10kHz.
4. This detector circuit readily permits miniaturization; with the possible exception of the two integrator capacitors.

Acknowledgement The authors want to thank Dr. H. M. Schlicke of the Allen-Bradley Company for his support, and Mr. R. Durisch, also of the Allen-Bradley Company; for the design of digital circuits for generating approximated sine and cosine waveforms.

References

1. ON THE TRANSMISSION OF INFORMATION BY ORTHOGONAL TIME FUNCTIONS, H. F. Harmuth, Transactions AIEE, Part I, Communication and Electronics, Vol. 79, July 1960, pp. 248-55.
2. COMPARISON OF PHASE COHERENT AND NON-PHASE COHERENT ODED COMMUNICATIONS, J. P. Strong and T. V. Saliga, Record of the 1965 International Space Electronics Symposium, pp. 5-A1 - 5-A8, Miami Beach, Florida, Dec. 1965.
3. SIGNAL DETECTION TECHNIQUES FOR A DISCRETE-FREQUENCY, PHASE-COHERENT PULSE FREQUENCY MODULATION (PFM) TELEMETRY SIGNAL, J. Y. Sos, Natl. Telemetry Conference Proceedings, pp. 252-255, Boston, Mass., May 1966.

4. STATISTICAL THEORY OF COMMUNICATION, K. W. Lee, J. Wiley and Sons, New York 1960, Chapter 12.
5. ELECTRONIC ANALOG AND HYBRID COMPUTERS, G. A. Korn, and T.M. Korn, McGraw-Hill Book Co., New York 1964.
6. THE ORTHOMATCH DATA TRANSMISSION SYSTEM, B. G. Kuhn, Lincoln Laboratory Report No. 346, AD602130, February 1964
7. KINEPLEX, A BANDWIDTH EFFICIENT BINARY TRANSMISSION SYSTEM, R. R. Mosier and R. G. Clabaugh. Transactions AIEEJ, Part I, Communciation and Electronics, Vol. 76, Jan. 1958, pp. 723-727.
8. Q AS A MATHEMATICAL PARAMETER, D. Morris, Electronic Engineer Vol. 26, July 1954, pp. 306-307.
9. HANDBOOK OF LAPLACE TRANSFORMATION, Floyd E. Nixon, Prentice Hall, Engelwood Cliffs, N.J., 1965, second edition; pages 185 (00.002), 211 (01.002)and 226 (02.002).

$e_1(t)/E$	$\cos 2\pi Nt/T$	$\sin 2\pi Nt/T$	$\cos 2\pi Mt/T$	$\sin 2\pi Mt/T$
$e_3(T)/\pi NE (R_0/R_1)^{\frac{1}{2}}$	1	0	0	0
$e_4(T)/\pi NE$	0	1	0	0

Table 1. Ideal values of $e_3(T)$ and $e_4(T)$. N, M integers, $N \neq M$; $\lambda = 0$, $\tau = T/2\pi N$.

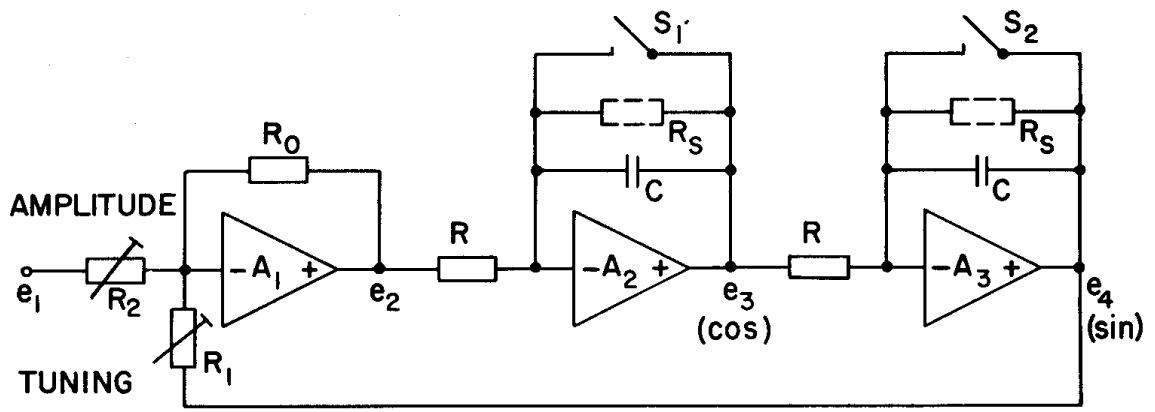


Fig. 1 Detector for orthogonal sine and cosine pulses

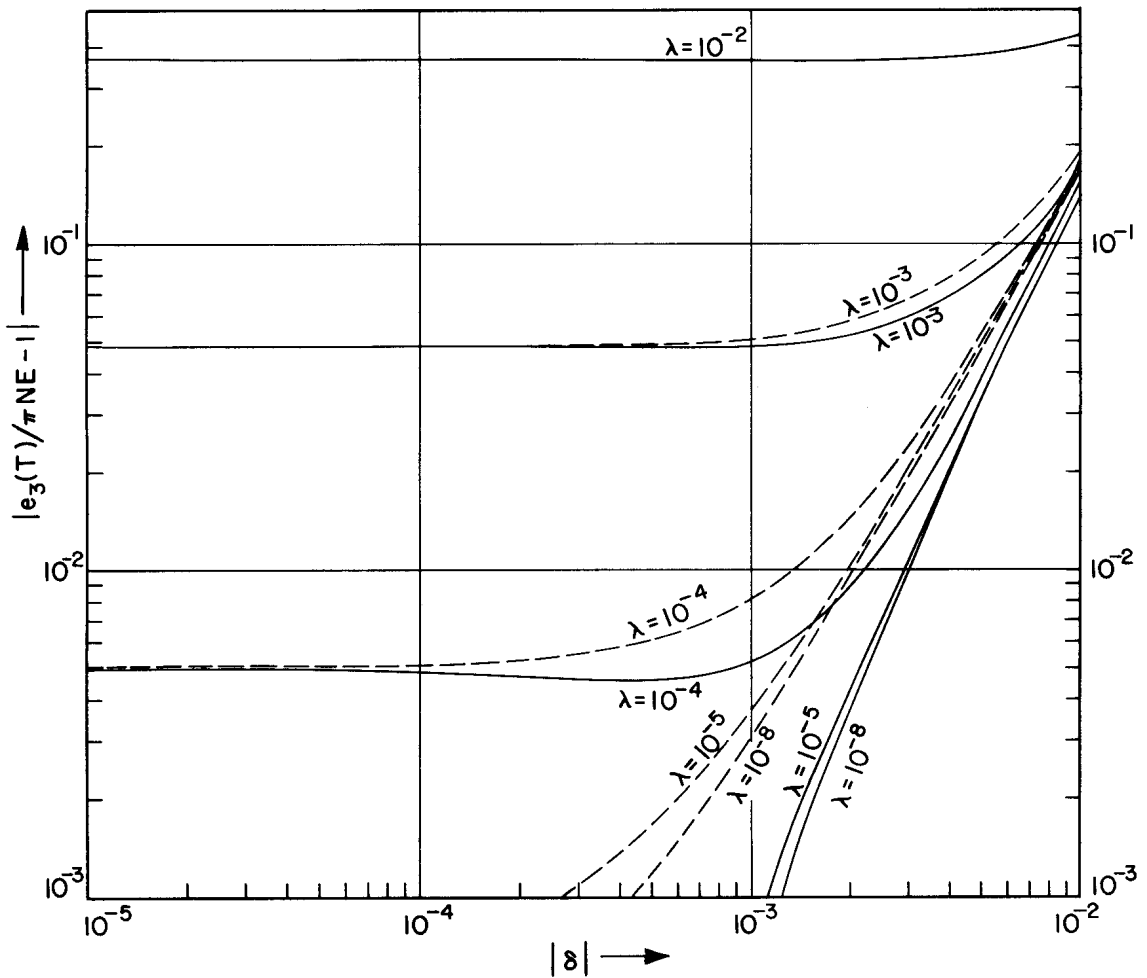


Fig. 2 $|e_3(T)/\pi NE - 1|$ as function of $|\delta|$ for $e_1(t) = E \cos 2\pi Nt/T$; $M = N = 16$.

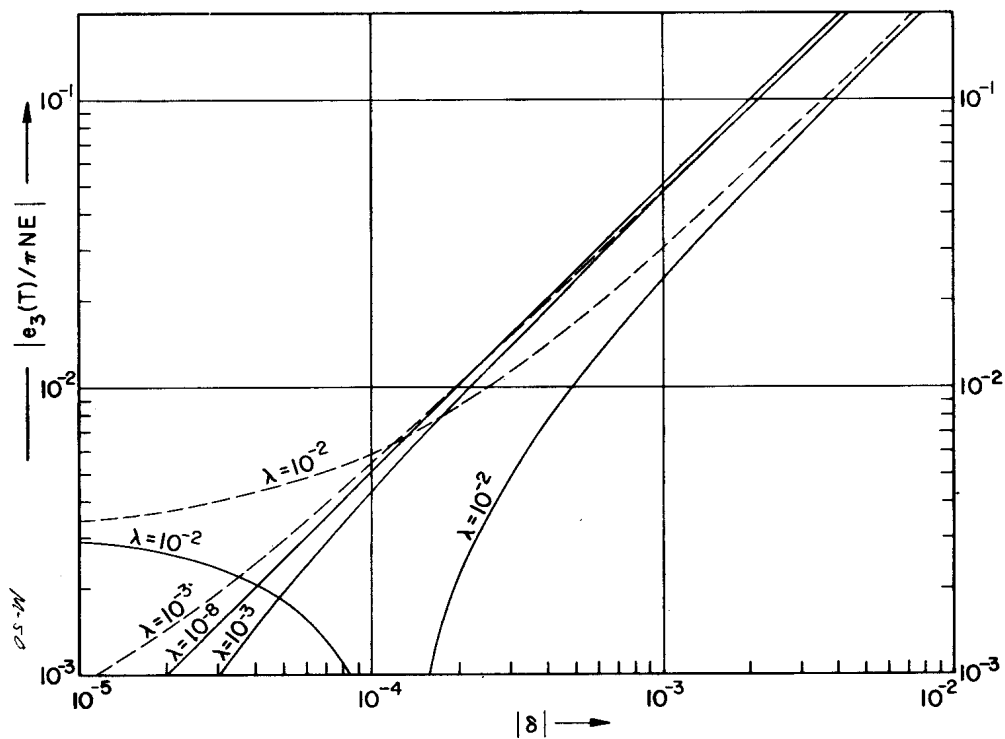


Fig. 3 $|e_3(T)/\pi NE|$ as function of $|\delta|$ for $e_1(t) = E \sin 2\pi Nt/T$;
 $M = N = 16$.

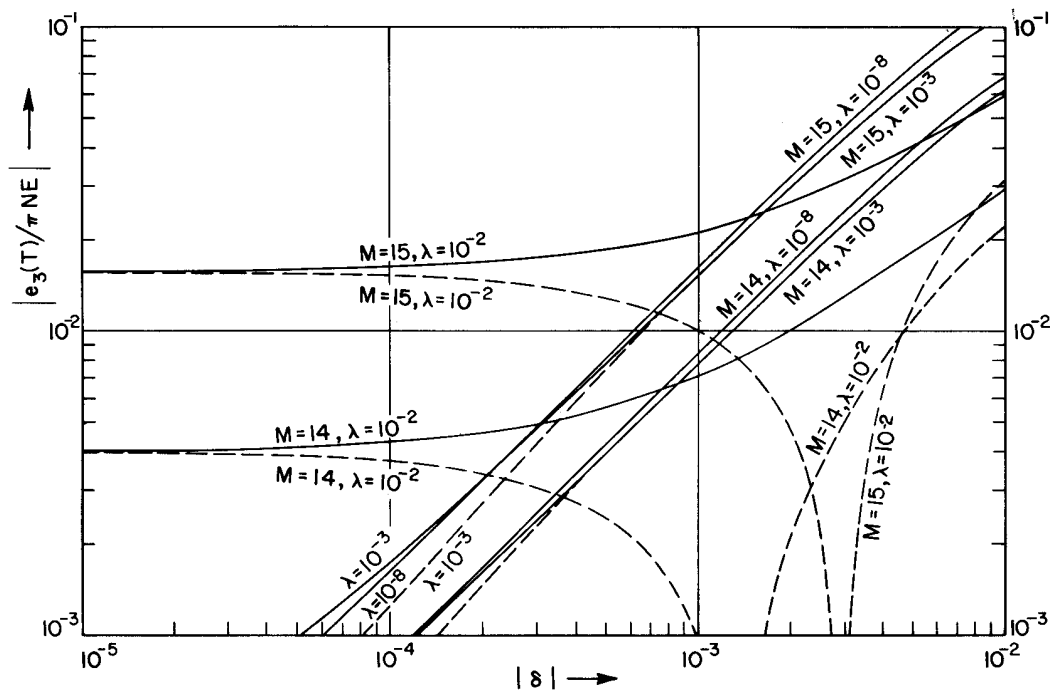


Fig. 4 $|e_3(T)/\pi NE|$ as function of $|\delta|$ for $e_1(t) = E \cos 2\pi Mt/T$;
 $N = 16$; $M = 14, 15$.

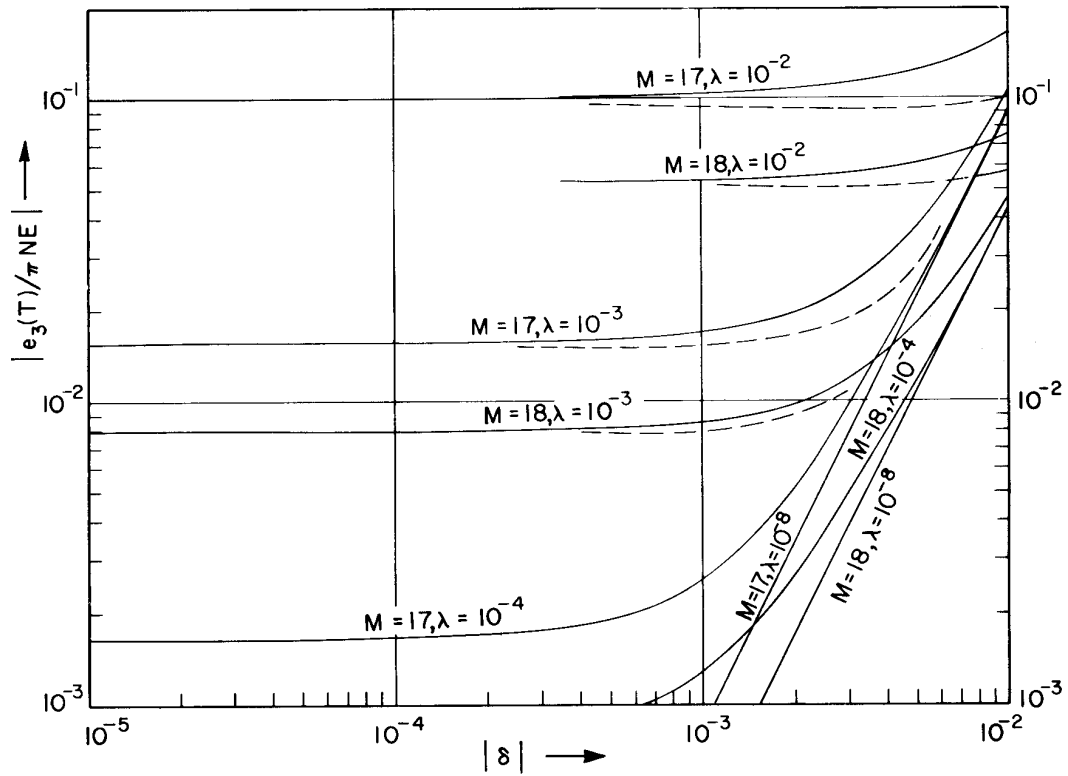


Fig. 5 $|e_3(T)/\pi NE|$ as function of $|\delta|$ for $e_1(t) = E \sin 2\pi Mt/T$; $N = 16$; $M = 17, 18$.

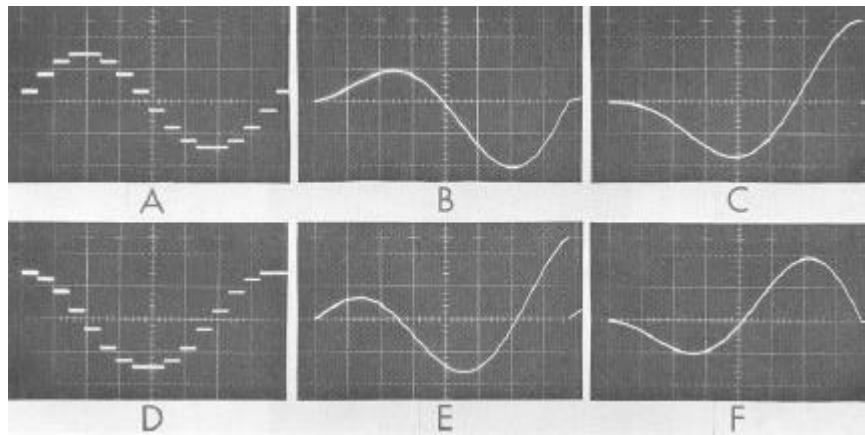


Fig. 6 Typical voltages of the circuit of Fig. 1. A: input voltage $e_1(t) = E \cos 2\pi t/T$; B and C: resulting output voltages $e_3(t)$ and $e_4(t)$; D: input voltage $e_1(t) = E \sin 2\pi t/T$; E and F: resulting output voltages $e_3(t)$ and $e_4(t)$.

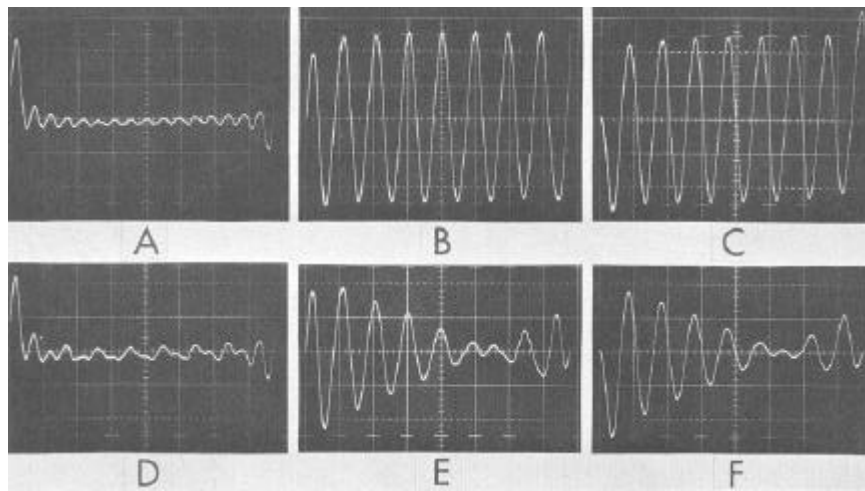


Fig. 7 Crosstalk from 30 orthogonal pulses into a detector tuned for $\tau = T/2\pi \cdot 8$; $T = 100$ ms; 1 vertical division = 2V.

A: $e_1(t) = E \sum_{M=1}^{16} [\cos 2\pi Mt/T + \sin 2\pi Mt/T]$

B: same as A, except that pulses with $M = 8$ are omitted.

C,D: $e_3(t)$ and $e_4(t)$ for input pulse A

E,F: $e_3(t)$ and $e_4(t)$ for input pulse B

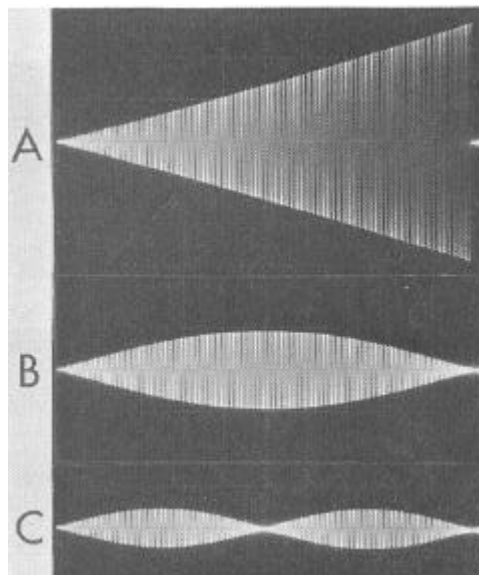


Fig. 8 Responses of three adjacent harmonic detectors to an input pulse

$e_1(t) = E \cos 2\pi \cdot 128t/T$ with $T = 8$ ms.

A: $e_3(t)$ at detector tuned for $\tau = T/2\pi \cdot 128$ (1024Hz)

B: $e_4(t)$ at detector tuned for $\tau = T/2\pi \cdot 129$ (1032Hz)

C: $e_4(t)$ at detector tuned for $\tau = T/2\pi \cdot 130$ (1040Hz)